*Proceedings of the Korean Nuclear Society Spring Meeting*
*Pohang, Korea, May 1999*

# Prediction of Critical Heat Flux in Highly Subcooled Flow Boiling with High Mass Velocity and Small Tube Diameter

**Young Min Kwon, DoHee Hahn**
Korea Atomic Energy Research Institute, ymkwon@nanum.kaeri.re.ke

**Soon Heung Chang**
Depart. of Nuclear Engineering, Korea Advanced Institute of Science and Technology

## Abstract

A phenomenological model based on wall-attached bubble coalescence, previously developed by the authors, was applied to predict a critical heat flux (CHF) in highly subcooled water flow boiling with high mass velocity and small tube diameter. A mechanistic approach to evaluate the profiles of flow quality and void fraction in the subcooled flow boiling was employed to take into account the enhanced condensation due to high subcooling in small diameter tubes. Comparison of the model predictions against 2938 subcooled water CHF data showed relatively good agreement over a wide range of parameters for fusion reactors operating conditions.

## 1. Introduction

A subcooled flow boiling of water is one of the most efficient and simplest techniques of removing high heat fluxes. However, successful uses of high-heat-flux subcooled flow boiling require that the critical heat flux (CHF) not to be reached. The CHF is one of the most important considerations in designing and performing safety analysis of nuclear reactors. Due to the necessity of the high heat flux removal from fusion reactor components, many studies of the CHF have recently been made under low pressures, high mass velocities, high subcooling, and relatively small tube diameters. The results of these studies were utilized to test the validity of the CHF models during subcooled flow boiling conditions.

According to the recent analyses made by Celata et al. [1] and Inasaka-Nariai [2, 3], existing correlations or models for subcooled flow boiling seem to lack the capability of accurately predicting the CHF in the conditions of fusion reactor operation. In spite of the intensive efforts of the CHF during subcooled flow boiling, all physical aspects causing this phenomenon are still not fully understood. The understanding is limited largely by the lack of experimental studies of a fundamental nature, which can be used for adequate theoretical models based on phenomenological mechanism.

The advantage of mechanistic model is that it would be easily improved and extended to a wide range of operating conditions, by modifying the relevant constitutive models, because of its mechanistic nature. However, no mechanistic model, as far as authors know, is applicable to a wide range of operating conditions applicable to both fission and fusion reactors. It is very difficult to properly model the CHF phenomena for a wide range of conditions, because most of existing models use empirical constants to adjust the model with the experimental data over the specific range.

The authors previously have developed a new CHF model [4, 5] based on the concept of wall-attached bubble coalescence and demonstrated their model could predict CHF in a wide range of flow conditions including subcooled and low quality conditions. The model was capable to predict CHF of non-aqueous fluids with reasonable accuracy [6]. The aim of the present paper is to evaluate its prediction performance for the high subcooling and high mass velocity conditions. A brief summary of the authors' previously developed CHF model is presented in the following section.

## 2. The CHF Model Based on Wall-Attached Bubble Coalescence

A physical image of the boiling structure considered is shown in Fig. 1, where the transverse interchange crossing the interface of the wall bubbly layer and core is shown. The effective thickness of bubbly layer is considered as a single bubble diameter, because it is assumed that only the wall-attached bubbles play the effective physical barrier to the heat transfer from the wall and the liquid supply from the core.

According to Saha and Zuber [7], at high mass flow rates, bubbles do not easily detach from their nucleation sites because bubbles are small enough to prevent detachment from the wall by the hydrodynamic forces. Therefore, the wall-attached bubbles form a wall bubbly layer, which acts as a wall roughness, with increasing the roughness of the tube. The existence of roughness changes the hydrodynamic characteristics of the flow and the effect of viscous shear due to molecular friction becomes relatively small. The frictional drag on the wall-attached bubbles depends upon the characteristic skin friction experienced by the wall bubbly layer. The CHF is assumed to reach at a certain void fraction in the wall bubbly layer (called critical wall-void fraction) when radial thermal transport is limited by equal flows inward and outward at the interface of the wall bubbly layer and core.

Based on the local phenomena hypothesis of the subcooled flow boiling CHF, governing equations are derived by applying the basic local conservation rules for mass, energy, and momentum to the control volumes such as that shown in Fig. 2. From total

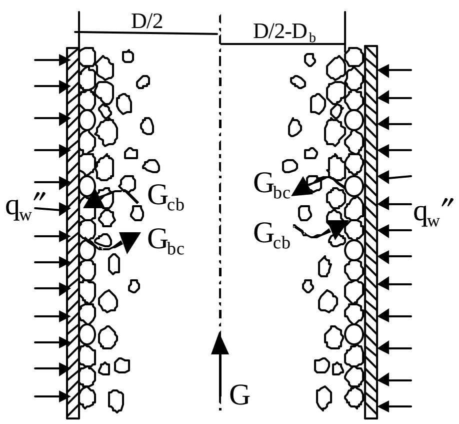


**Fig. 1** Conceptual configuration of bubbles on the heated wall.

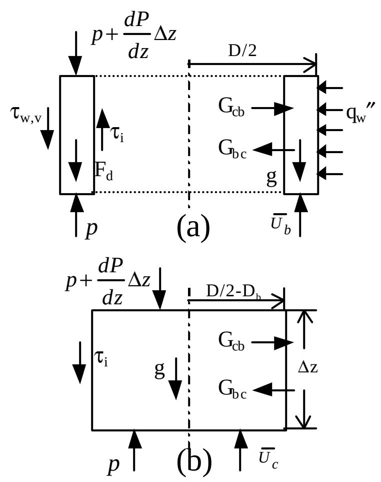


**Fig. 2** Separated flow control volumes for (a) wall bubbly layer and (b) core.

mass and energy balances on the wall bubbly layer of Fig. 2(a), the CHF formula of Eq. (1) is derived.

$$q''_w = G^*(h_b - h_c)\frac{\xi_i}{\xi_w} \tag{1}$$

$G^*$ is the limiting transverse interchange of mass flux at the interface of the wall bubbly layer and core, which is obtained from the momentum balance equations on the control volumes of the wall bubbly layer and core, respectively.

$$G^* = \left[\left(\rho_c - \rho_b\right)g + \frac{\pi D F_d}{D_b^2(1-\eta_c)A}\right]\left[\frac{A\eta_c(1-\eta_c)}{(\overline{U}_c - \overline{U}_b)\xi_i}\right] \tag{2}$$

In Eq. (2), $F_d$ is the frictional drag that the rough element of a single bubble exerts on the flow field. As a first approximation, the drag force exerted on a single bubble is assumed to be $F_d=\lambda\rho_c U_c^2/2\times(\pi D_b^2/4)$, which is the same approach as done in Staub's [8] subcooled boiling model. The critical wall-void fraction $\alpha_b$ was approximately correlated by the relation of Eq. (3), which is only valid for $\alpha_{avg} > 0.8$.

$$\alpha_b = 0.83 - 0.29\exp\left(-4.71x_{em} - 1.89\right) \tag{3}$$

The correlation of Eq. (3) was obtained by fitting against total 5009 data points. The parameter ranges of experimental data are: $1 \le D \le 37.5$ mm, $0.035 \le L \le 6$ m, $450 \le G \le 7500$ kg/m$^2$s, $2 \le P \le 20$ MPa, $0 \le \Delta h_{sub,in} \le 1660$ kJ/kg, and $0.135 \le q_{CHF} \le 14.8$ MW/m$^2$, most of which data are low quality saturate condition. Among those data points, only 892 out of 5009 points belong to subcooled conditions at the tube exit

Reliable predictions of the detached bubble diameter are of essential for the prediction of CHF. The Levy [9] model is employed to predict the point of onset of bubble departure (OBD) and the bubble departure diameter. The turbulent skin friction coefficient $\lambda$ is calculated using the Colebrook-White equation with a two-phase Reynolds number to account for the variation of the fluid viscosity near the heated wall. The average viscosity of core is evaluated by Beattie and Whalley [10]. The universal velocity profile for a single-phase turbulent flow proposed by Karman is assumed to be valid in the turbulent core. The average fluid velocity of the wall bubbly layer is determined by taking it as half the velocity of the core at the outer edge of the wall bubbly layer. The flow quality and void fraction in the subcooled flow boiling can be evaluated by the simple profile-fit method of Saha and Zuber [7] and Dix [11] model, respectively. All equations utilized in the present model are presented in Appendix I of Ref. 5.

## 3. CHF Prediction for High-Heat-Flux Subcooled Flow Boiling

According to Celata [12], the thermal hydraulic conditions of fusion reactor components are such as high subcooling (up to 250 K), high mass flux (greater than 10 Mg/m$^2$s), small-intermediate tube diameter (1-15 mm), low-intermediate pressure (up to 5 MPa), and very high heat flux (up to 80 MW/m$^2$). The CHF under the condition of typical fusion reactor components may be different from that under the regular subcooled flow boiling condition. In order to extend the authors' previously developed CHF model to fusion reactor operating conditions, a mechanistic method to evaluate the flow quality and void fraction in subcooled flow boiling was employed to take account for the enhanced condensation due to high subcooling in small diameter tubes.

### 3.1 Flow Quality Profile Model in Subcooled Convective Boiling

There are two distinctly different approaches to predict the flow quality and void fraction in subcooled flow boiling; a profile-fit method and a mechanistic method. The profile-fit method is fully empirical, while the mechanistic method satisfies some conservation laws but still uses empirical relations for closure. The profile-fit method is easier to use than the mechanistic method and is as accurate in normal steady case. The mechanistic model may have insufficient data to accurately specify the basic mechanism involved, but it does afford a valid functional form of the basic physics involved. One of the important issues in developing accurate mechanistic model for high subcooling and high flow rate conditions is the accurate estimation of the condensation rate.

In the author's previous work, the flow quality was evaluated by the simple profile-fit model of Saha and Zuber [7]. Because little difference in the CHF predictions appeared for low subcooled and low positive quality conditions when both approaches were employed. The relationship between the true flow quality $x_{avg}$ and the thermodynamic equilibrium qualities is expressed by Eq. (4),

$$x_{avg} = \frac{x_{em} - x_d \exp\left(x_{em}/x_d - 1\right)}{1 - x_d \exp\left(x_{em}/x_d - 1\right)} \tag{4}$$

where $x_d$ and $x_{em}$ are thermodynamic equilibrium qualities determined at the onset of bubble departure (OBD) point and at the tube exit, respectively. The location of OBD is the most important parameter in Eq.(4), which is evaluated by the Levy [9] model.

For the high-heat-flux subcooled flow boiling with high mass velocity and small tube diameter, which is the focus of this paper, Nariai and Inasaka [13] reported that much lower void fraction was observed than the prediction by the profile-fit model. They considered that the difference of void fraction was caused by intense condensation effect for the small diameter tubes with high liquid velocity. However, actually no satisfactory models for enhanced condensation in small diameter tubes exists in the present time, which is understandable in view of the complexity of the turbulence induced condensation process.

In the subcooled flow boiling, the heat flux at the heating wall is typically partitioned into that required to generate vapor, that associated with single-phase convection, and that due to liquid agitation or pumping. Bowring [14] defined a pumping factor, ε, which is the ratio of the heat flux due to pumping to that causing vapor generation, and used an empirical correlation for its estimation. Rouhani and Axelsson [15] neglected the single-phase convection component based on the assumption that the heating wall was fully covered by bubbles downstream of the OBD point and considered the pumping component only. Then they defined the pumping factor in the form of Eq.(5).

$$\varepsilon = \frac{\rho_l \left(h_f - h_l\right)}{\rho_g h_{fg}} \tag{5}$$

The resulting expression for flow quality between the OBD and the interesting point along the heated flow path was given by Lahey and Moody [16]

$$x_{avg} = \frac{1}{GAh_{fg}} \left\{ \int_{z_d}^{z} \frac{P_H q_b'' dz}{[1+\varepsilon]} - \int_{z_d}^{z} P_H q_{cond}'' dz \right\} \tag{6}$$

where $P_H$ is the heated perimeter and the net boiling heat flux $q_b''$ is given by :

$$q_b'' = q_w'' \left\{ 1 - \left[ \frac{h_{ls} - h_{lc}}{h_{ls} - h_{ld}} \right] \right\} \quad \text{for} \quad h_l \geq h_d \qquad \text{or} \qquad q_b'' = 0 \quad \text{for} \quad h_l < h_d \tag{7}$$

As a first step for taking into account the condensation effect on the CHF, a first order model can be used to test the physics of the condensation. The condensation heat flux is given by a functional relationship, experimentally determined by Levenspiel [17], such as:

$$q_{cond}'' = 270 \frac{h_{fg} \rho_{fg}}{P_H} A \alpha_{avg} (T_{sat} - T_l) \quad \text{for} \quad h_l \geq h_d \qquad \text{or} \qquad q_{cond}'' = 0 \quad \text{for} \quad h_l < h_d \tag{8}$$

where the constant value of 270 $(h^{o}C)^{-1}$ was fitted by the experimental void data. An iterative approach is required to calculate $x_{avg}$ at the tube exit. The whole procedure to calculate the CHF is shown in Fig.3.

### 3.2 Experimental High-Heat-Flux CHF Data

Among the total of 5009 experimental CHF data used for fitting of Eq. (3) in the previous work, only 892 data points have subcooled condition at the tube exit, and most

**Table 1.** Experimental CHF data for subcooled flow boiling.

| Parameter<br>Reference | No. | D<br>(mm) | L<br>(m) | P<br>(MPa) | G<br>(Mg/m²s) | $\Delta h_{in}$<br>(kJ/kg) | $q''_{CHF}$<br>(MW/m²) |
|---|---|---|---|---|---|---|---|
| Thompson et al. [24]* | 541 | 1.14 ~ 37.5 | 0.01 ~ 1.97 | 0.1 ~ 19.6 | 0.66 ~ 29.4 | 50.0 ~ 1659 | 0.94 ~ 37.7 |
| Becker et al. [25]* | 114 | 6.0 ~ 10.0 | 0.15 ~ 3.0 | 0.15 ~ 20.0 | 0.45 ~ 14.90 | 271 ~ 1372 | 0.64 ~ 35.6 |
| Zenkevich [26]* | 245 | 5.8 ~ 11.0 | 0.22 ~ 4.0 | 3.86 ~ 19.6 | 0.96 ~ 5.06 | 183 ~ 1617 | 1.28 ~ 7.72 |
| Chen et al. [18] | 109 | 10.0 ~ 16.0 | 0.15 ~ 3.0 | 0.16 ~ 20.0 | 0.4 ~ 13.4 | 228 ~ 1384 | 1.36 ~ 14.56 |
| Boyd [19,20, 21]** | 28 | 10.2 | 0.5 ~ 1.17 | 0.45 ~ 1.6 | 0.76 ~ 7.45 | 544 ~ 772 | 1.39 ~ 11.5 |
| Nariai et al. [22] | 14 | 6.0 | 0.1 | 0.1 ~ 5.12 | 4.87 ~ 10.05 | 245 ~ 1017 | 8.5 ~ 27.77 |
| Celata et al. [1] | 1887 | 0.33 ~ 2.54 | 0.002 ~ 0.61 | 0.09 ~ 8.41 | 0.92 ~ 90.0 | 88 ~ 1018 | 3.33 ~ 228 |
| Total | 2938 | 0.33 ~ 37.5 | 0.002 ~ 4.0 | 0.1 ~ 20.0 | 0.4 ~ 90 | 50 ~ 1659 | 0.64 ~ 228 |

* 892 out of total 902 data were used for fitting of Eq. (3)

** Data not included in ENEA database

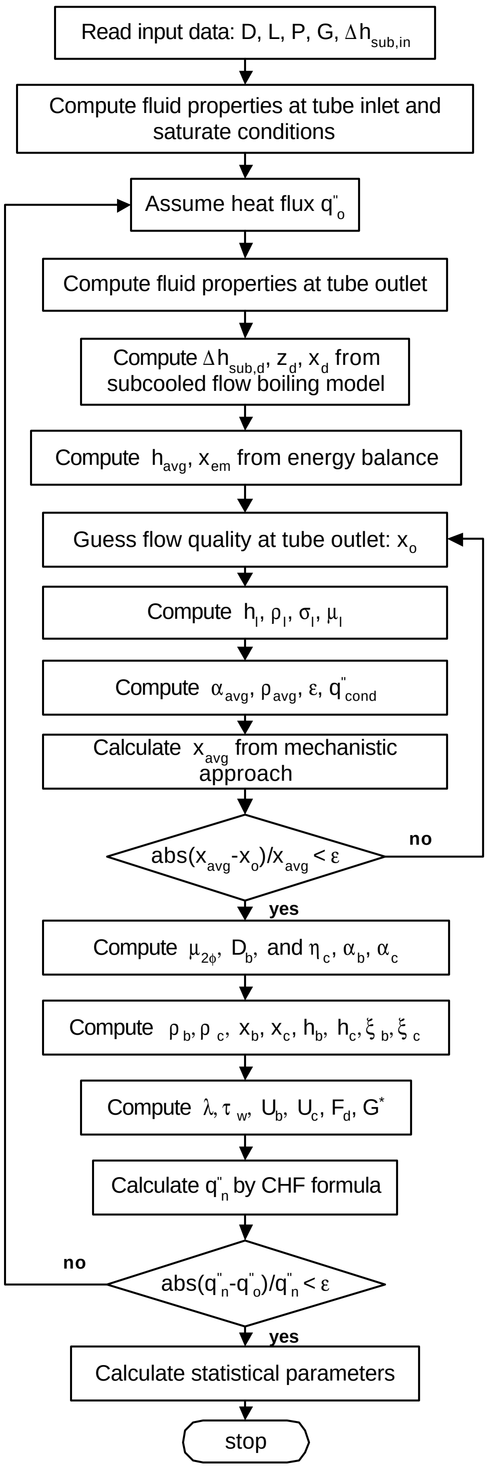


Fig.3 CHF calculation procedure

of which are categorized into the regular subcooled flow boiling condition applicable to LWRs. In order to investigate the effects of condensation in small diameter tubes with high mass velocity, some experiments have been conducted. To assess the predictive capabilities of the proposed CHF predictive procedure, a total of 2938 CHF data points for water flow in uniformly heated round tubes was obtained from different sources. The ENEA CHF database, composing of 1888 data points, in the range of fusion reactor thermal hydraulics was collected by Celata et al. [1] from twenty-five sources. Recent data sets of Chen et al. [18], Boyd [19, 20, 21], and Nariai et al. [22] were included in the present database. The data of Boyd were obtained from horizontal tube test, however the effect of tube orientation was negligible because of high mass velocity. The range of parameters for each data source, considered in this study, is presented in Table 1. The parameter ranges are: $0.3 \le D \le 37.5$ mm, $0.002 \le L \le 4$ m, $0.1 \le P \le 20$ MPa, $0.4 \le G \le 90$ Mg/m$^2$s, $50 \le \Delta h_{sub,in} \le 1659$ kJ/kg, and $0.64 \le q''_{CHF} \le 228$ MW/m$^2$, which covers the operating ranges of typical fusion reactor components.

Ornatskii and Vinyarskii [23] obtained CHF higher than 200 MW/m$^2$ under the conditions of G=90 Mg/m$^2$s, P≈3 MPa, $\Delta T_{sub,in}$≈200 K, D=0.5 mm, L=14 mm. The CHF mechanism under these extreme conditions may be largely different from those governed in the LWRs. Nariai and Inasaka [13] systematically investigated the effect of tube diameter and tube length on the CHF. Experiments were conducted at nearly ambient pressure under conditions: D=1, 2, 3 mm; L=1, 3, 5, 10 cm; G=7000, 13000, 20000 kg/m$^2$s; inlet water temperature $T_{in}$=20, 60 °C. The abnormality of the subcooled flow boiling in the narrow tubes with high velocity was found. The actual void fraction for the narrow tubes with high liquid velocity became considerably different from those estimated by the existing correlations or models. Nariai and Inasaka reported that, for D=1 mm and G=13000 kg/m$^2$s, the estimated void fraction was about 70% of theoretical prediction by the Ahmad model [27]. For D=1 mm and G=20000 kg/m$^2$s, estimated void fraction was about 45% of theoretical one. The reduced void fraction at the tube exit resulted in increase of the CHF.

Following the results of Nariai and Inasaka [13], the present CHF database was simply classified into two categories based on tube inside diameter. However, the actual value for this boundary could not be clarified. The first category dealing with the CHF data of D < 3 mm includes 1038 out of 2938 data points. Among them 246 data points have less than 1 mm inside diameter. The second category of D ≥ 3 mm includes remaining 1900 data points.

### 3.3 Model Prediction and Discussion

The Prediction performance of the CHF model was quantitatively evaluated by the CHFR, defined as the ratio of the predicted to measured CHF, with three statistical parameters of $\mu$ (average value), $\sigma$ (sample standard deviation), and RMS (root-mean-square error) of CHFR. The comparisons were conducted for two tube diameter ranges of D < 3 mm and D ≥ 3 mm.

Figs. 4-5 show the visual comparison of the predicted and measured CHF for each range, respectively. The symbol N in the plots means the number of experimental data that successfully predicted by the model. For small diameter tubes, the comparison results in Fig. 4 show a relatively large discrepancy and the proposed procedure underestimated the CHF with $\mu$=0.93, RMS=23.9%, and $\sigma$=22.7%. While for D ≥ 3 mm range, the proposed procedure predicted fairly well as shown in Fig. 5, most of the experiment data were predicted within ±30% error band with $\mu$=1.05, RMS=14.6%, and $\sigma$=13.9%. As tube inside diameter decreases and mass flow rate increases, the detachment bubble diameter becomes smaller, which is governed by the Levy [9] model. Furthermore it can be expected that intense condensation by the transverse interchange mass flux ($G_{cb}$) of highly subcooled water made the wall-attached bubbles small. Then small void fraction made the CHF larger. It should be noted that, for some data points in the ENEA data set, the mechanistic flow quality model predicted higher average bulk void fraction larger than 0.8 at the tube exit. As is known, the prediction accuracy by the proposed CHF model deteriorates when the average void fraction exceeds 0.8.

The percentage of data points calculated with the corresponding error band (±%) is presented in Fig. 6. The effects of the flow quality model in subcooled flow boiling for both ranges are shown in the figure. Generally, the mechanistic method predicted higher CHF than the profile-fit method. Especially, for small diameter tubes the profile-fit method gave much underestimated values ($\mu$=0.87). The results of mechanistic method were better than the profile-fit one for this range. This is mainly a consequence of a large condensation effect. While for D ≥ 3 mm range, even though no considerable difference on the prediction results between two methods was shown in Fig. 6, the profile-fit method results were slightly better than the other one. The prediction results by the Celata et al. [28] model are included in the same figure. For small tube diameter, the Celata et al. model seemed to give most reasonably predictions.

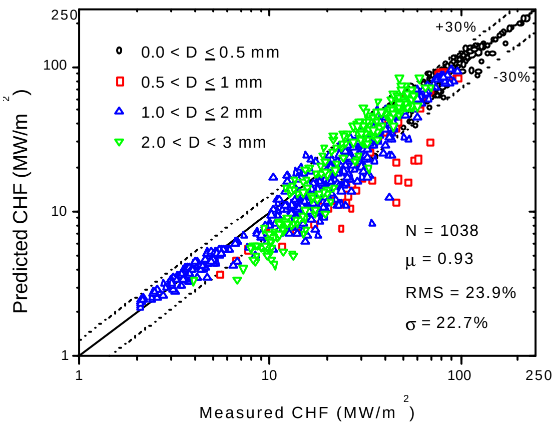


**Fig. 4** Predicted vs measured CHF for D < 3 mm.

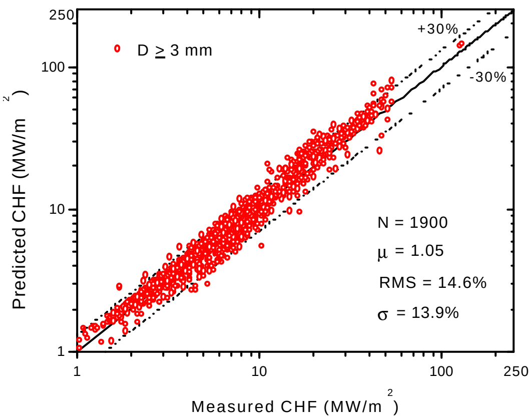


**Fig. 5** Predicted vs measured CHF for D ≥ 3 mm.

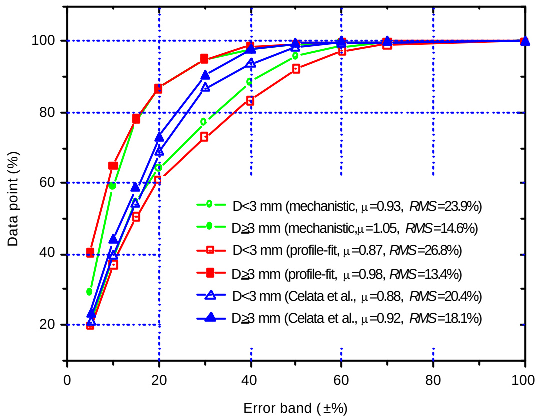


**Fig. 6** Percentage of data points predicted within error band by the proposed and Celata et al. models.

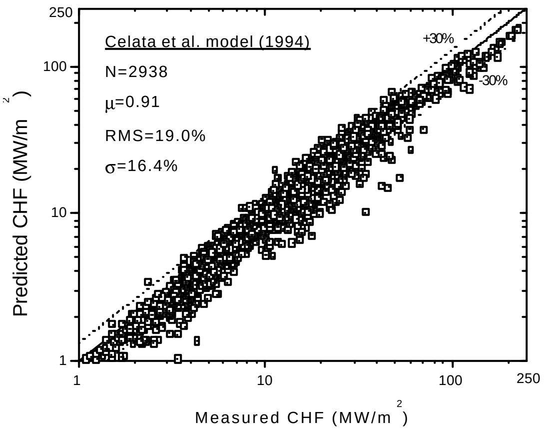


**Fig. 7** CHF predictions by the Celata et al. model (1994b).

Fig. 7 shows a visual comparison of predictions by the Celata et al. model with 2938 experimental data points. About 89% of data points were predicted within ±30%, with μ=0.91, RMS=19.0%, and σ=16.4%. While the proposed procedure predicted about 89% of the data within ±30%, with μ=1.00, RMS=18.4%, and σ=18.4%. This statistical result of prediction performance is not bad, considering the wide application ranges of the proposed CHF model. Although the ranges of the present database were out of the recommended range of Eq.(3), the proposed procedure predicted the CHF with relatively good statistical results for high-heat-flux subcooled flow boiling.

The dependence of the prediction accuracy (CHFR) on major parameters is presented in Figs. 8-11, where the CHFR is plotted versus pressure, mass flux, inlet subcooling, and tube inside diameter, respectively. The comparison of the predictions by the CHF model with experimental data exhibited systematic deviations on the pressure for small diameter tube range. The model has a tendency to underpredict CHF for low pressure (P < 0.5 MPa) and low inlet subcooling conditions. While, no significant systematic effects on the model predictions are shown for the range of D ≥ 3 mm.

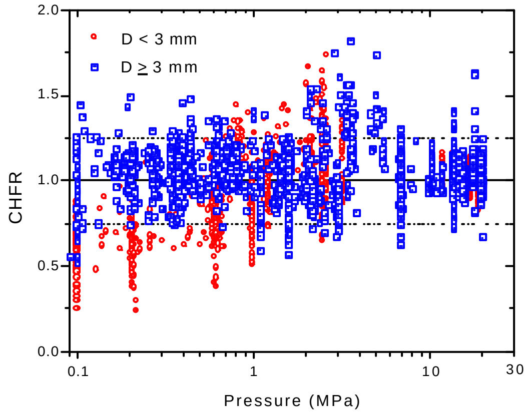


**Fig. 8** CHFR vs pressure.

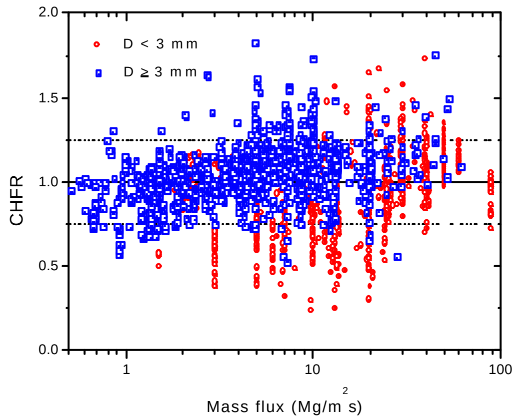


**Fig. 9** CHFR vs. mass flux.

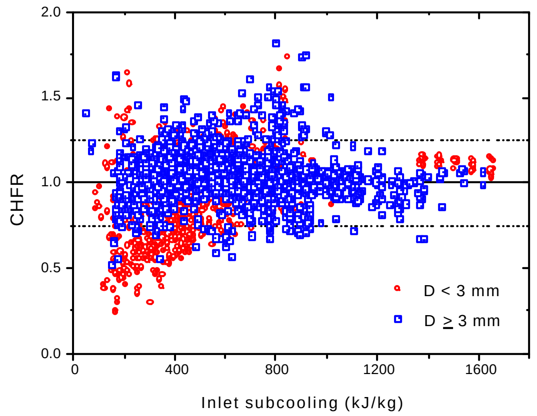


**Fig. 10** CHFR vs inlet subcooling.

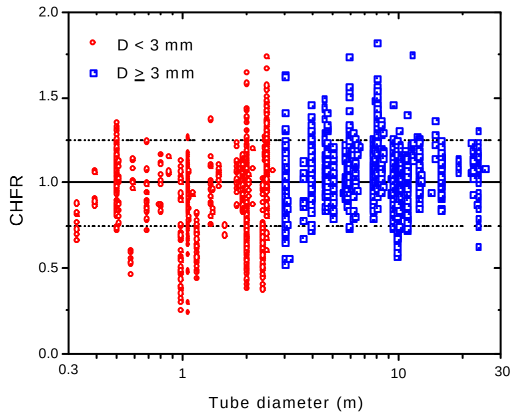


**Fig. 11** CHFR vs. tube diameter.

The recent CHF data sets of Boyd [19, 20, 21], Inasaka-Nariai [29], Nariai et al. [22], Vandervort et al. [30], Celata et al. [31] and Chen et al. [18] were specially selected for the assessment of the proposed prediction procedure. The data of Inasaka-Nariai, Vandervort et al., Celata et al, and Boyd are included in the ENEA database. Fig. 12 shows the comparison results of prediction by the proposed procedure.

## 4. Conclusion

The CHF model proposed by the authors has been tested on the wide range of subcooled flow boiling condition. A total 2938 data points covers the operating ranges of typical fusion reactor components: $0.3 \le D \le 37.5$ mm, $0.002 \le L \le 4$ m, $0.1 \le P \le 20$ MPa, $0.374 \le G \le 90$ Mg/m$^2$s, $50 \le \Delta h_{sub,in} \le 1659$ kJ/kg, and $0.64 \le q''_{CHF} \le 228$ MW/m$^2$. Although the database is beyond of the application of the previously developed model, the comparison of the predicted CHF against the database showed relatively good performance, about 89% of data points were predicted within ±30% error band with RMS=18.4%, and $\sigma$=18.4%. This statistical result is not bad, considering the wide application ranges of the proposed predictive procedure. For tube diameter being greater than 3 mm, the model predicted fairly well, with $\mu$=1.05, RMS=14.6%, and $\sigma$=13.9%.

However, although an enhanced condensation effect was considered in the mechanistic flow quality model, a considerable underprediction of the CHF was shown for several data sets with very small diameter tubes (D < 3 mm). The constitutive models that employed in the construction of the proposed CHF model might not hold for small tube diameter at high mass velocity. Taking into account the reduction of void fraction in such extreme conditions, improved theoretical models to evaluate the profiles of flow quality and void fraction are required.

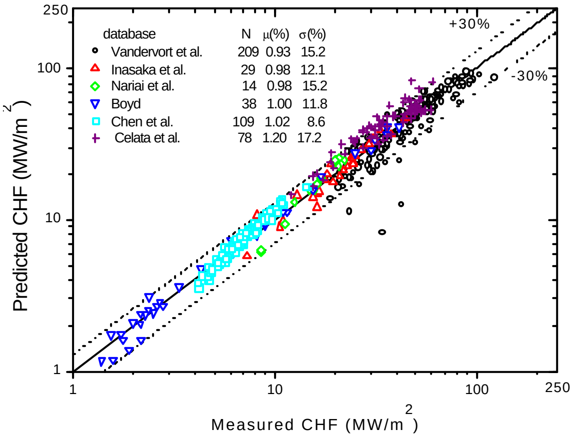


**Fig. 12** Predicted vs measured CHF. for selected data sets.

## Nomenclature

| | |
|---|---|
| $A$ | cross-section area ($m^2$) |
| $D$ | tube diameter (m) |
| $D_b$ | detached bubble diameter (m) |
| $F_d$ | drag force on a single bubble (N) |
| $G$ | mass flux ($kg/m^2s$), |
| $G^*$ | limiting transverse mixing mass flux ($kg/m^2s$) |
| $g$ | acceleration due to gravity ($m/s^2$) |
| $h$ | enthalpy (kJ/kg) |
| $\Delta h$ | degree of subcooling (kJ/kg) |
| $h_{fg}$ | latent enthalpy of vaporization (kJ/kg) |
| $P$ | pressure (MPa) |
| $q''$ | heat flux ($kW/m^2$) |
| $\overline{U}$ | mean velocity (m/s) |
| $x$ | quality |
| $x_{em}$ | thermal equilibrium quality at tube exit |
| $\alpha$ | void fraction, |
| $\eta_c$ | fraction of cross-section occupied by core |
| $\lambda$ | skin friction coefficient |
| $\mu$ | viscosity ($Ns/m^2$) |
| $\rho$ | density ($kg/m^3$) |
| $\sigma$ | surface tension (N/m) |
| $\tau_w$ | apparent wall shear stress ($N/m^2$) |
| $\tau_{w,v}$ | viscous shear stress on wall ($N/m^2$) |

### Subscripts

| | |
|---|---|
| avg | average |
| b | bubbly layer |
| bc | from bubbly layer to core |
| c | core |
| cb | from core to bubbly layer |
| f | saturated liquid |
| g | saturated vapor |
| i | interface of bubbly layer and core |
| in | inlet |
| l | liquid phase |
| w | heated wall |

## Acknowledgement

This work was performed under the Long-term Nuclear R&D Program sponsored by the Korea Ministry of Science and Technology.

## References

1. Celata, G.P., Cumo, M., Mariani, A., Assessment of correlations and models for the prediction of CHF in water subcooled flow boiling, *Int. J. Heat Mass Transfer* **37**, 237-255 (1994).
2. Inasaka, F., Nariai, H., Evaluation of subcooled critical heat flux correlations for tubes with and without internal twist tapes, *Nucl. Eng. Des.* **163**, 225-239 (1996).
3. Inasaka, F., Nariai, H., Evaluation of subcooled flow boiling CHF based on the mechanistic models for high mass velocity and high subcooling conditions, Proc. of NUTHOS-5, Beijing, China, Paper AA2 (1997).
4. Kwon, Y.M., Chang, S.H., A mechanistic critical heat flux model for subcooled flow boiling using a rough-wall analogy of wall-attached bubbls, 2nd Int. Symp. on Two-Phase Flow Modelling and Experimentation, Pisa, Italy (1999).
5. Kwon, Y.M. Chang, S.H., An improved mechanistic model to predict critical heat flux in subcooled and low quality forced convection boiling, *J. Korean Nucl. Society* **31** (1999).
6. Kwon, Y.M., Chang, S.H., A mechanistic critical heat flux model for wide range of subcooled and low quality flow boiling, Nucl. Eng. Des. (accepted for publication)
7. Saha, P., Zuber, N., Point of net vapor generation and vapor void fraction in subcooled boiling, Proc. 5th Int. Heat Transfer Conf., Tokyo, Japan, Vol. IV, pp.175-179 (1974).
8. Staub, F.W., The void fraction in subcooled boiling - prediction of the initial point of net vapor generation, J. Heat Transfer **90,** 151-157 (1968).
9. Levy, S., Forced convection subcooled boiling - prediction of vapor volumetric fraction, *Int. J. Heat Mass Transfer* **10**, 951-965 (1967).
10. Beattie, D.R.H., Whalley, P.B., A simple two-phase frictional pressure drop calculation method, Int. J. Multiphase Flow **8**, 83-87 (1982).
11. Dix, G.E., Vapor void fractions for forced convection with subcooled boiling at low flow rates, NEDO-10491, General Electric Company (1971).
12. Celata, G.P., Critical heat flux in subcooled flow boiling, Proc. of 11th Int. Heat Transfer Conf., Kyongju, Korea, Vol.1, pp.261- 277 (1998).
13. Nariai, H., Inasaka, F., Critical heat flux and flow characteristics of subcooled flow boiling with water in narrow tubes, Jones, O.C. and Michiyoshi, I. (Ed), *Dynamics of Two-Phase Flows*, CRC Press, pp.689-708 (1992).
14. Bowring, R.W., Physical model based on bubble detachment and calculation of steam voidage in the subcooled region of a heated channel, Report HPR-10, Inst. For Atomenergi, Halden, Norway (1962).
15. Rouhani, S.Z., Axelsson, E., Calculation of void volume fraction in the subcooled and quality boiling region, *Int. J. Heat Mass Transfer* **13**, 383-393 (1970).
16. Lahey Jr, R.T., Moody, F.J., The Thermal-Hydraulics of a Boiling Water Nuclear Reactor, American Nuclear Society, 2nd edn., La Grange Park, Illinois, Chapter 5 (1993)

17. Levenspiel, O., Collapse of steam bubbles in water, *Ind. Eng. Chem*. **51** (1959).
18. Chen, Y., Zhou, R., Hao, L., Chen, H., Critical heat flux with subcooled boiling of water at low pressure, 8th Int. Topical Meeting on Nuclear Reactor Thermal-Hydraulics, Kyoto, Japan, Vol.2, pp.958-964 (1997).
19. Boyd, R.D., Subcooled water flow boiling experiments under uniform high heat flux conditions, *Fusion Technology* **13**, 131-142 (1988).
20. Boyd, R.D., Subcooled water flow boiling at 1.66 MPa under uniform high heat flux conditions, ASME Winter Annual Meeting, HTD Vol.119, pp.91-15 (1989).
21. Boyd, R.D., Subcooled water flow boiling transition and the L/D effect on CHF for a horizontal uniformly heated tube, *Fusion Technology* **18**, 317-324 (1990).
22. Nariai, H., Inasaka, F., Kinoshita, H., Critical heat flux of subcooled flow boiling with and without internal twisted tape under circumferentially non-uniform heating condition, Proc. German-Japanese Sympo. on Multiphase Flow, pp.191-205 (1994).
23. Ornatskii, A.P., Vinyarskii, L.S., Heat transfer crisis in a forced flow of underheated water in small-bore tubes, *High Temperature* **3**, 400-406 (1965).
24. Thompson, B., Macbeth, R.V., Boiling water heat transfer in uniformly heated round tubes: A compilation of world data with accurate correlations, AEEW-R-356 (1964).
25. Becker, K.M., Strand, G. et al., Round tube burnout data for flow of boiling water at pressure between 30 and 200 bar, Report KTH-NEL-14 (1971).
26. Zenkevich, A., Analysis and generalization of experimental data on heat transfer crisis associated with forced convection of cooling water in tubes, AECL-Tr-Misc-304 (1974).
27. Ahmad, S.Y., Axial distribution of bulk temperature and void fraction in a heated channel with inlet subcooling, *Trans. ASME, J. Heat Transfer* **92**, 595-609 (1970).
28. Celata, G.P., Cumo, M., Mariani, A., Simoncini, M., Zummo, G., Rationalization of existing mechanistic models for the prediction of water subcooled flow boiling critical heat flux, *Int. J. Heat Mass Transfer* **37**, suppl.1, 347-360 (1994).
29. Inasaka, F., Nariai, H., Critical heat flux of subcooled flow boiling for water in uniformly heated straight tubes, *Fusion. Eng. Des.* **19**, 329-337 (1992).
30. Vandervort, C.L. Bergles, A.E., Jensen, M.K., An experimental study of critical heat flux in very high heat flux subcooled boiling, Int. J. Heat Mass Transfer **37**, 161-173 (1994).
31. Celata, G.P., Cumo, M., Mariani A., Burnout in highly subcooled water flow boiling in small diameter tubes, *Int. J. Heat Mass Transfer* **36**, 1269-1285 (1993).